Selective Excitation in High-Resolution NMR

RAY FREEMAN

Department of Chemistry, Cambridge University, Cambridge, England

Contents

I. Introduction

In the days when high-resolution NMR spectroscopy was performed by slow-passage continuous-wave methods there was little need for special techniques for selective excitation, all experiments were inherently selective. It was only when pulse methods began to gain the acendency that this question had to be addressed in a serious manner. Nevertheless, a start had already been made in the pioneering work of Alexander[1] who devised a method for pulsed excitation of one resonance while leaving a chemically shifted neighbor unaffected (subjected to 2π radians rotation). Pulse experiments were not really needed for high-resolution work until interest was kindled in relaxation[2,3] and slow chemical exchange studies[4] in spectra of many lines. This approach seemed less exciting when the Fourier transform revolution[5] made it possible to make relaxation measurements on all the resonances in the high-resolution spectrum in a set of time-dependent experiments.[6]

Fourier transform spectrometers offered so many advantages that the original slow passage methods were essentially abandoned in the span of a few years. However, there was one thing that the Fourier method

could not handle very well—the intense signal from proton solvents such as water. Even heavy water presented difficulties (from residual HDO) when dilute solutions of biomolecules were under investigation. The large dynamic range spanned by the solvent and solute signals exceeded the capabilities of the analog-to-digital converter, introducing "digitization noise" that was very unwelcome indeed. This provided the impetus for a whole family of solvent-suppression techniques[7] that often used a frequency-selective pulse.[8]

The vast majority of high resolution spectroscopists were concerned only with the excitation of the entire spectral width ΔF in a uniform manner—they required "hard" pulses in the sense

$$\gamma B_1 / 2\pi \gg \Delta F$$

A pioneering few were experimenting with "soft" pulses where $\gamma B_1 / 2\pi$ was of the order of a typical line width $\Delta \nu$ or a coupling constant J (in hertz). These are sometimes called "line-selective" and "multiplet-selective" pulses, respectively. Much more recently there have been experiments designed to excite a selected range of chemical shifts without perturbing the rest of the spectrum; these are known as "band-selective" pulses. With these distinctions, a hard pulse has a clear definition, but a soft pulse could mean one of several things.

Ray Freeman was born in Long Eaton, England in 1932. He did his undergraduate (M.A.) and graduate studies (D. Phil.) at Oxford University, followed by postdoctoral work with Professor Abragam in Paris. He has worked at the National Physical Laboratory, Teddington, England; Varian Associates, Palo Alto, CA; the Physical Chemistry Laboratory and Magdalen College, Oxford, and is now John Humphrey Plummer Professor of Magnetic Resonance at Cambridge University. His research interests are in new techniques in high-resolution nuclear magnetic resonance, particularly multidimensional spectroscopy.

II. Selective Pulses

The simplest and most straightforward selective excitation method is to use a single, low-amplitude radiofrequency pulse of relatively long duration. In the early experiments this would be a rectangular pulse. It needs to be variable in frequency and preferably independent of the frequency of the proton transmitter. The proton decoupler channel can be useful here. For a typical multiplet-selective experiment, the radiofrequency level would be set to satisfy the conditions

$$|\nu_A - \nu_X| \gg \gamma B_1/2\pi > |J_{AX}|$$

where X has the closest chemical shift to the nucleus A under investigation.

We may regard the criterion for frequency selectivity in two ways. In the vector picture, a pulse is selective because the B_1 field is weak; once the offset ΔB becomes comparable with B_1 then the effective field in the rotating frame is appreciably tilted with respect to the x axis and the magnetization vector will not reach the xy plane after a $\pi/2$ pulse. The selectivity is therefore of the order of $\gamma B_1/2\pi$ Hz. The pulse must have a long duration t_p in order to satisfy the condition

$$\gamma B_1 t_p = \pi/2$$

Alternatively, we could argue that pulses of long duration are inherently selective by analogy with the Heisenberg principle.

The basic properties of soft pulses can be illustrated in a very simple experiment performed on a continuous-wave NMR spectrometer.[2,3] Excitation is by means of a field modulation sideband response with the modulation frequency chosen to be high enough (kilohertz) that the centerband and all save one of the sidebands lie outside the spectral region. Pulsing merely involves switching the audiomodulation to give a pulse width of the order of 100 ms to 1 s. Even mechanical switches and relays are fast enough for the purpose, although electronic gating is preferable. The great advantage of this scheme is that the NMR signal may be observed not only after but also *during the pulse*. This makes pulse-width calibration a simple matter, for a π pulse would show an NMR response in the form of the first half cycle of a sine wave. Phase shifts, such as that required in the Meiboom–Gill modification,[9] are implemented as audiofrequency phase shifts. The transmitter runs continuously and is neither gated nor shifted in phase; indeed no radiofrequency modifications are needed at all.

A. Spin–Lattice Relaxation

This scheme allows the selective investigation of relaxation times of individual lines in a high-resolution spectrum one at a time. Spin–lattice measurements employ the usual inversion recovery sequence

$$- T - \pi - \tau - \pi/2 \text{ (acquire)}$$

where T is chosen to be long compared with all relaxation times. Alternatively, the complete time evolution of longitudinal magnetization can be followed in an experiment employing 2π pulses to monitor the nuclear magnetization

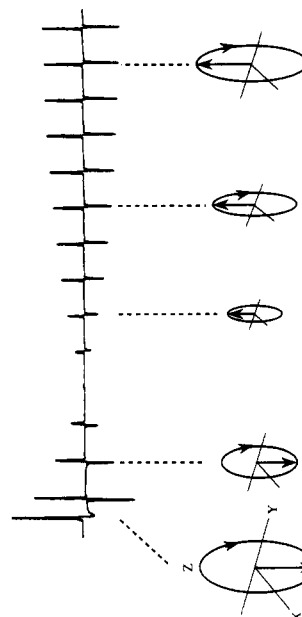$$- T - \pi - \tau - 2\pi - \tau - 2\pi - \tau \dots$$

Figure 1. Spin–lattice relaxation measured by means of soft audiofrequency pulses where the signal may be observed during the pulse. After population inversion by a π pulse, the recovery of z magnetization is monitored (as a single cycle of a sine wave) by a series of 2π pulses.

where the NMR response is observed (as a single cycle of a sine wave) during the 2π pulses. Figure 1 shows a spin–lattice recovery curve monitored by this method.

Transient nuclear Overhauser effects[10] or slow chemical exchange[4] may be initiated with a selective π pulse on one resonance while the intensity change of a neighbor resonance is monitored with a $\pi/2$ pulse. More sophisticated applications involve the study of nonexponential relaxation in coupled-spin systems[11,12] where information can be obtained about the degree of correlation between the external fields due to a paramagnetic entity responsible for spin–lattice relaxation. For solutions of small molecules where the spin–lattice relaxation times are many tens of seconds, these experiments are particularly simple to perform.

B. Spin–Spin Relaxation

Spin–spin relaxation may be monitored through a Carr–Purcell[13] sequence with multiple refocusing and the Meiboom–Gill phase shift[9]

$$- T - (\pi/2)_x - \tau - (\pi)_y - \tau - \text{echo} - \tau - (\pi)_y - \tau \dots$$

An example of the use of soft pulses to measure proton spin–spin relaxation times in 2,3,4-trichloronitrobenzene[2] is shown in Figure 2. The two aromatic protons signals decay at quite different rates (T_2 = 2.0 and 7.9 s) because one is coupled to a nitrogen nucleus that is rapidly relaxed through its quadrupolar interaction. Note that selective spin–spin relaxation measurements in homonuclear-coupled systems afford some important advantages over hard-pulse methods. In the soft-pulse experiment there are no complications due to modulation by spin–spin coupling.

Another technique for spin–spin relaxation studies in coupled spin systems is the spin-locking experiment[14] since, for these selective experiments, the continuous B_1 field is of low amplitude and there is little power dissipation. Spin echoes in the rotating frame[15] may
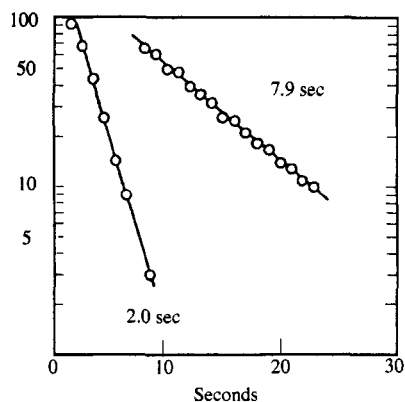
Figure 2. Selective pulse spin–spin relaxation study of the two protons in 2,3,4-trichloronitrobenzene by the audiofrequency pulse method. Each decay curve is measured in a separate experiment, the signal intensity being plotted on a semilogarithmic graph, the slope giving T_2. The faster relaxing proton is the one next to the nitro group.

also be implemented in a straightforward fashion by using an audiofrequency phase inverter to refocus the effects of spatial inhomogeneity of the B_1 field. In general, spin–spin relaxation studies are much more susceptible to instrumental shortcomings than experiments with spin populations.

C. The Overhauser Effect

One example of the application of a soft multiplet-selective pulse is the determination of the degree to which protons in a sugar derivative are relaxed by the dipole–dipole mechanism. Although this information can be obtained from steady-state nuclear Overhauser measurements, in multispin systems these may be complicated by three-spin effects and spillover of saturation onto nearby resonances. A multiplet-selective pulse scheme allows the dipolar contribution to be assessed by a quite different technique, the comparison of the rate of recovery of a chosen multiplet after selective inversion with the corresponding recovery rate after non-selective inversion of the entire spectrum.[10]

The theory can be most simply followed by treating a coupled two-spin system with four energy levels. The equilibrium spin populations may be represented as in Figure 3a. The transition probabilities are defined as W_1, W_2, and W_0 for dipole–dipole interactions and $W_1{}^*$ for all other mechanisms. The rate equations describing the recovery from a general perturbation may then be written

$$\mathrm{d}n_1/\mathrm{d}t = (n_2 - n_1)(W_1 + W_1{}^*) + $$
$$(n_3 - n_1)(W_1 + W_1{}^*) + (n_4 - n_1)W_2$$

$$\mathrm{d}n_2/\mathrm{d}t = (n_1 - n_2)(W_1 + W_1{}^*) + (n_3 - n_2)W_0 + $$
$$(n_4 - n_2)(W_1 + W_1{}^*)$$

$$\mathrm{d}n_3/\mathrm{d}t = (n_2 - n_3)W_0 + (n_1 - n_3)(W_1 + W_1{}^*) + $$
$$(n_4 - n_3)(W_1 + W_1{}^*)$$

$$\mathrm{d}n_4/\mathrm{d}t = (n_2 - n_4)(W_1 + W_1{}^*) + $$
$$(n_3 - n_4)(W_1 + W_1{}^*) + (n_1 - n_4)W_2$$

Consider first the case of a *nonselective* 180° pulse which inverts the populations of all four transitions. The resulting *deviations from equilibrium* are shown in Figure 3b. Since the populations n_1 and n_4 are heavily involved, the double-quantum transition prob-
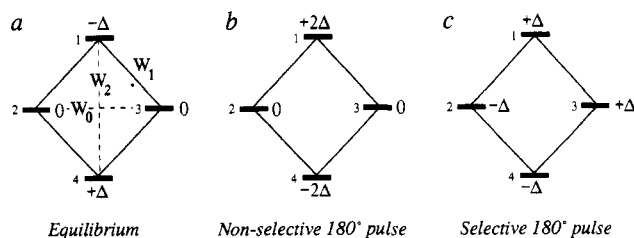

Figure 3. (a) Spin populations at Boltzmann equilibrium in a two-spin system. (b and c) The deviations from equilibrium population caused by 180° pulses. After a population disturbance such as b, it is clear that relaxation will be predominantly influenced by the W_2 transition probability, characteristic of the dipole–dipole interaction.

ability W_2 features strongly in the population dynamics. The rate equation is

$$\mathrm{d}(n_1 - n_2)/\mathrm{d}t = 2\Delta(W_1 + W_1{}^* + W_2)$$

For a selective 180° pulse the population deviations from equilibrium are as shown in Figure 3c. The corresponding rate equation is

$$\mathrm{d}(n_1 - n_2)/\mathrm{d}t = \Delta(2W_1 + 2W_1{}^* + W_2 + W_0)$$

Consequently the ratio of the nonselective rate to the selective rate is given by

$$K = 1 + (W_2 - W_0)/(2W_1 + 2W_1{}^* + W_2 + W_0)$$

With the usual nomenclature

$$\rho = 2W_1 + W_2 + W_0 \qquad \rho^* = 2W_1{}^*$$
$$\sigma = W_2 - W_0$$

the ratio K may be written

$$K = 1 + \sigma/(\rho + \rho^*)$$

When the dipole–dipole mechanism is completely dominant then ρ^* may be neglected in comparison with ρ and

$$K = 1 + \sigma/\rho = 1.5$$

This is the maximum nuclear Overhauser enhancement for protons. If there is "leakage" through other relaxation mechanisms (ρ^*) then K lies between 1.0 and 1.5.

This technique was tested on the 100-MHz spectrum of the protons in a glucopyranose derivative.[10] The nonselective experiment was carried out with a hard 180° pulse in the usual manner (Figure 4a). A soft 180° pulse was used in the selective experiment to invert H1, leaving all other protons unaffected. In this case the relaxation is noticeably slower (Figure 4b). Since it is no longer a strictly exponential curve (the other protons slowly deviate from Boltzmann populations) only the initial rate is measured. This gave a ratio $K = 1.5$ confirming that the relaxation mechanism is predominantly a dipole–dipole interaction with the other protons in the molecule. This conclusion is corroborated by conventional nuclear Overhauser experiments on the same sample.

D. Solvent Peak Suppression

In the old continuous-wave frequency-sweep spectrometers an intense solvent peak could be simply truncated and no particular harm would be done. In Fourier transform spectrometers, excessive demands are made on the digitization process when the signals span a large dynamic range. The problems arise from nonlinearity of the receiver, computer memory overflow,
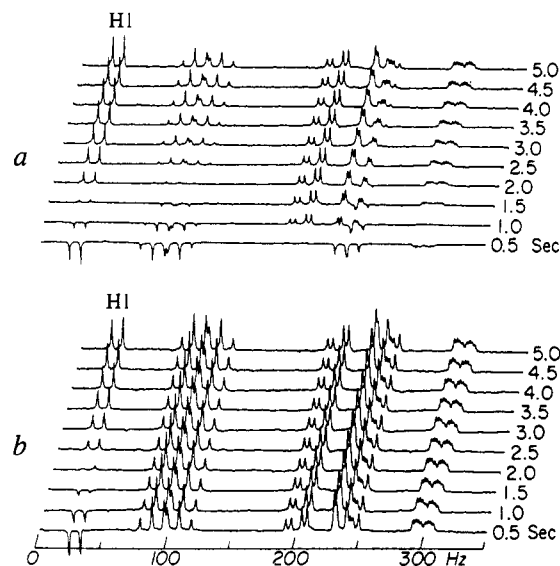
Figure 4. Spin–lattice relaxation of protons in a glucopyranose derivative after a nonselective π pulse (a) and after a selective π pulse (b) applied to H1. The ratio of the initial rates of recovery of the H1 signal in a and b can be used to evaluate the nuclear Overhauser effect due to the other protons in the molecule (reprinted from ref 10; copyright 1974 American Institute of Physics).

Fourier transformation round-off errors and, most serious of all, limitations in the dynamic range of the analog-to-digital converter. The worst situation arises with dilute aqueous solutions of biomolecules where the H_2O peak is 10^5 times more intense than a millimolar solute resonance. Even in cases where heavy water can be used, the residual HDO line is still very strong. The spectrometer gain has to be reduced to the point where the analog-to-digital converter does not clip the strong solvent resonance. This often means that the weak signals of interest are comparable with the digitization noise which arises through Fourier transformation of the small digitization errors.

An amazing number of ingenious schemes have been proposed to counter these problems. They can be roughly divided into those that force the solvent peak to be near a null condition (by saturation or inversion-recovery) and those that avoid exciting the solvent at all. Of the latter, a selective excitation scheme is quite common, leaving the water magnetization vector along the z axis but exciting the rest of the spectrum. A combination of a hard and a soft pulse may be used, but the problem is that the tails of the strong water resonance extend to appreciable offsets where the soft pulse is less effective. Redfield[8] has devised a composite soft pulse (214) that has the advantage of providing a relatively broad null response. Guéron[16] introduced the "jump and return" sequence, $(+\pi/2) - \tau - (-\pi/2)$ where the free precession interval τ allows off-resonance spins to dephase before the final pulse. Signals close to the solvent are perturbed in intensity and are inverted on one side of the spectrum. This pulse sequence, which may be written 1:$\bar{1}$, was soon followed by others based on the binomial coefficients—the 1:$\bar{2}$:1 sequence[17] and the 1:$\bar{3}$:3:$\bar{1}$ sequence[18,19] which have a broader null condition. Tolerance of instrumental imperfections is particularly important; these include spatial inhomogeneity of the B_1 field, inaccurate phase shifts, imbalance between the different phase channels, radiation damping and relaxation during the pulse. Hore[20] has ana-

lyzed these problems and concludes that phase-alternating binomial sequences are the most promising and that, of these, the 1:$\bar{3}$:3:$\bar{1}$ pulse is probably the best compromise between performance and simplicity.

E. Resolution Enhancement

Selective pulses play an important role in magnetic resonance imaging. For example, the first stage of many imaging experiments is slice selection; the excitation of spins in the narrow region between two parallel planes through the sample. This is usually accomplished by applying a frequency-selective pulse in the presence of a strong static field gradient in a direction normal to these planes. All other spins in the sample are too far from resonance for significant excitation. These ideas can also prove useful in high-resolution NMR spectroscopy for resolution enhancement. In principle, we could always sacrifice sensitivity and improve resolution by reducing the size of the NMR sample, for then the line width due to spatial inhomogeneity should decrease. In practice such an improvement is seldom achieved. The reason is that smaller samples still need to be confined within some kind of container, and the discontinuities on bulk magnetic susceptibility at the container walls distort the applied field appreciably, so that an irreducible "hard core" line width remains.

However, it is possible to enhance resolution by decreasing the *effective* sample volume and this can be achieved by adapting the selective pulse techniques of magnetic resonance imaging. For many high-resolution situations it is the longitudinal (z) gradient that is most critical, for its effect is not improved by sample spinning. Suppose that we deliberately apply a field gradient in the z direction while exciting with a selective pulse. Only a flat disk-shaped region of the sample will be excited, its volume depending on the intensity of the gradient and the selectivity of the pulse. The gradient is then extinguished before signal acquisition. Free precession occurs in the usual static field inhomogeneity but since the effective sample volume is greatly restricted in the z direction, z gradients now have far less influence. The method is easily demonstrated by performing experiments with increasingly strong applied z gradients, thereby progressively reducing the effective sample volume and improving resolution. Figure 5 shows some typical results for an imperfectly resolved spin multiplet of furan-2-aldehyde.[21] Note that the signal-to-noise ratio decreases as the resolution increases, as expected.

III. The DANTE Sequence

With the Fourier transform spectrometers of the 1970s it was rather inconvenient to generate a soft radiofrequency pulse. Facilities for switching the radiofrequency level were often lacking, and fine-tuning of the transmitter frequency was not always feasible. A simpler solution was to apply a regular train of n hard pulses of small flip angle β arranging to make $n\beta = \pi/2$ or π radians, depending on the application. This DANTE sequence[22,23] is most easily described in terms of the vector picture of NMR in the rotating reference frame. At exact resonance the effect of the n hard pulses is cumulative, and the magnetization moves in a smooth arc from the $+z$ axis to $+y$. The method owes
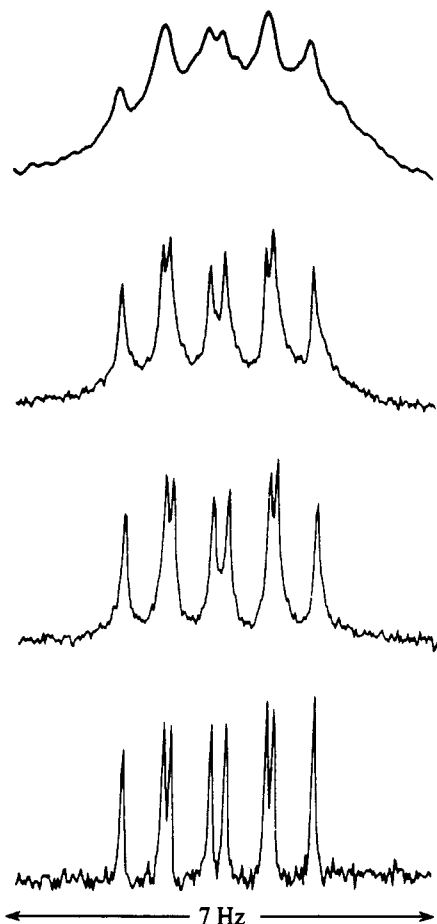
Figure 7. Magnetization trajectories for a selective pulse at four different offsets from exact resonance. Owing to the increasing tilt of the effective field in the rotating frame, the path of the magnetization curves progressively further from the zy plane as the offset increases. The corresponding DANTE trajectories approximate the same curves in the limit of high pulse repetition rate.
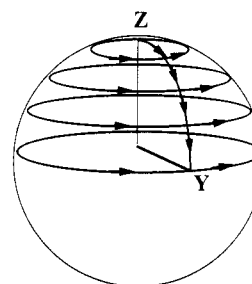
Figure 8. The first sideband response of a DANTE sequence occurs when the offset from resonance is such as to allow a complete 2π rotation about the z axis in the interval between pulses. The overall result is similar to that of the centerband response.

Figure 5. Resolution enhancement by selective excitation in an applied field gradient. A spin multiplet of furan-2-aldehyde has been excited in increasingly strong gradients, giving resolution that increases from 0.6 Hz (top) to 0.08 Hz (bottom). As the effective volume decreases the sensitivity is reduced (reprinted from ref 21; copyright 1980 Academic Press).
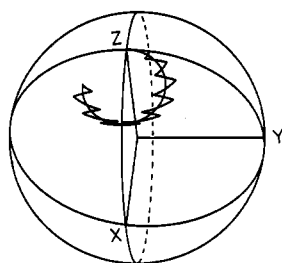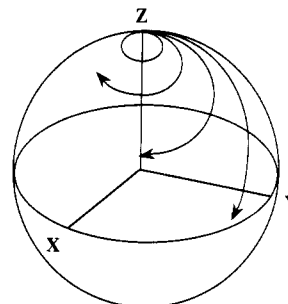

Figure 6. A typical zigzag magnetization trajectory of a DANTE sequence made up of only nine pulses, compared with the corresponding smooth trajectory of a single soft pulse.

its selectivity to the fact that at an offset Δf from resonance, free precession occurs through a small angle $2\pi\Delta f\tau$ radians in the interval τ between hard pulses. The trajectory is then a zigzag path that curves away from the zy plane. Figure 6 illustrates a typical zigzag DANTE trajectory and the corresponding trajectory for a single soft pulse of duration $n\tau$ seconds and a reduced transmitter level. DANTE is essentially the time-shared version of a single soft pulse. At high enough pulse repetition rates the zigzag displacements are small and the DANTE trajectory can be approximated as a smooth curve. Figure 7 shows a typical family of magnetization trajectories at increasing offsets from resonance, neglecting the small zigzag deviations. When Δf is large, the trajectories reduce to a series of small

cyclic excursions near to the $+z$ axis and the excited signal is weak. Frequency selectivity is controlled by the overal duration $n\tau$ of the sequence.

There is, however, an important distinction between DANTE and a single soft pulse. Not only is there strong excitation at the transmitter frequency (the centerband response) but also at a series of sideband conditions ($\tau\Delta f = k$) where the spins accomplish a whole number k of complete revolutions about the z axis in the interval τ (Figure 8). This has an important practical advantage. If we work with a sideband response (say $k = +1$), fine tuning of the exact resonance condition is achieved by adjusting τ^{-1}, the pulse repetition rate. DANTE therefore provides a convenient control of overall flip angle, selectivity, and excitation frequency. It also has the practical advantage of employing the same transmitter system for both selective and nonselective pulses, avoiding possible problems with phase synchronization between two different transmitters.

Usually in a DANTE sequence the number of pulses n is chosen in the range 10–100; if it is too high the individual pulse widths become impractically short. Pulse shaping is simply implemented by modulating the hard pulse flip angles according to an appropriate function. Most modern selective pulse experiments may be implemented in practice either as a single low-intensity pulse or as the corresponding DANTE sequence.

Some applications demand excitation at more than one frequency simultaneously. Although it is possible to add together two DANTE sequences with different repetition rates, the experimental implementation is complicated by occasional coincidences and near-coin-
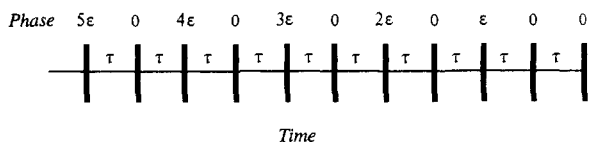
Figure 9. Interleaving of two DANTE sequences with equal repetition rates $1/(2\tau)$ Hz. One has a constant phase angle for all pulses; the other has a phase angle that rotates progressively in very small steps of ϵ radians each. This permits selective excitation at two independently adjustable frequencies separated by $\epsilon/(2\tau)$ rad/s.
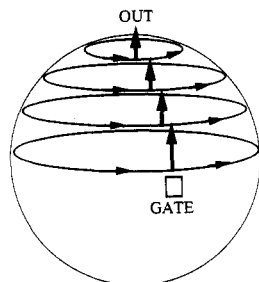

Figure 10. Schematic diagram of the path prescribed for souls in Dante's *Purgatory*. Note the similarity, apart from a trivial reversal of sign, with the trajectories illustrated in Figure 8.

cidences of the pulses.[23] A better scheme[24] is to interleave two DANTE sequences of the same repetition rate, $1/(2\tau)$ Hz. One sequence has all pulses of the same phase, while the other progressively increments the phase in small steps of ϵ radians. We may think of this combination as two independent DANTE sequences (Figure 9), each operating in its own rotating reference frame with angular frequencies differing by $\epsilon/(2\tau)$ rad/s. The y axes of the two frames are timed to come into coincidence at the end of the interleaved sequence (unless we wish the two excitations to have different phases).

Gareth Morris[23] noticed that a trajectory made up of a sequence of small jumps and 2π rotations bears a close analogy with the path prescribed for souls in Dante's *Purgatory*, illustrated schematically in Figure 10. This is the origin of the DANTE acronym (delays alternating with nutations for transient excitation). As is often the case in science, the DANTE sequence was discovered by accident in the pursuit of a quite different goal.[25] The idea was to devise a simple test for short spin–spin relaxation times in multiline high-resolution spectra by performing a sequence of 2π transient nutations just prior to the $\pi/2$ excitation pulse. If the 2π rotations are exact, they have no net effect on the conditions just prior to the $\pi/2$ pulse, except for relaxation, which proceeds at a rate

$$1/T = \tfrac{1}{2}(1/T_1 + 1/T_2)$$

In the usual situation where $T_1 = T_2$ the loss of magnetization would be quite modest, but if T_2 is short the loss could be appreciable. Comparison of line intensities in experiments with and without transient 2π nutations should therefore indicate which chemical sites had short relaxation times. The experiment was tested on the carbon-13 spectrum of o-dichlorobenzene where the ortho carbon sites were known to have shorter spin–spin relaxation times than the meta and para positions. The first test of the nutation method went well, and the resonance of the C–Cl groups lost intensity with respect to the C–H groups, as expected. A fol-

low-up experiment on a different spectrometer completely contradicted this finding, one of the C–H groups losing intensity while the C–Cl group remained unaffected. In analyzing this disaster we came to the conclusion that the pulse length calibration must have been slightly at fault.[25] The regular sequence of "2π" pulses was acting as a train of small flip angle pulses, giving selective excitation at a frequency determined by the (arbitrary) repetition rate. This new application promised to be far more useful than the original relaxation test.

IV. Tailored Excitation

One of the first attempts to devise a really general method of selective excitation was the experiment proposed by Tomlinson and Hill.[26] It assumes a Fourier transform relationship between the pulse modulation envelope and the frequency-domain excitation profile. Thus in principle it allows the operator to specify any arbitrary excitation profile and then calculate the pulse scheme to implement it, hence the name "tailored excitation". The frequency-domain excitation pattern is defined (in terms of amplitude and phase) at a large number of discrete points, equally spaced in frequency. For example, if we require band-selective excitation, most of these components would be zero, with just a few adjacent channels containing appreciable intensities. For practical reasons associated with the dynamic range limitations of the modulator, the phases are then scrambled by a pseudorandom sequence. A discrete Fourier synthesis is then carried out to give the waveform for modulating the pulse widths from the radiofrequency transmitter. Instrumental shortcomings in the modulation scheme may limit the fidelity of reproduction of the theoretical excitation pattern. Of perhaps more concern is the fact that the Fourier relation is only an approximation, strictly valid only for conditions where the spin response is linear. In retrospect, these limitations appear to have restricted the usefulness of tailored excitation, for in practice it proved incapable of generating a sharp step function in the excitation profile, such as would be needed for band-selective experiments. Nevertheless these experiments alerted the NMR community to the possibilities of multiplet-selective and band-selective excitation in high-resolution NMR.

V. Shaped Pulses

A. Gaussian

As selective pulses were applied to practical problems it soon became apparent that a rectangular-shaped pulse is far from ideal. In the frequency domain, the central excitation peak is flanked by an extensive pattern of sidelobes which decrease in intensity with offset. This sinc function character can be understood (in the Fourier approximation) as the transform of the rectangular pulse envelope. It seems that these step-function discontinuities need to be smoothed out if the sidelobes are to be eliminated from the excitation profile. One of the first shaping functions to be tried was a Gaussian.[27,28] There is a theorem, based on the Fourier approximation, which states that a shaping function that can be differentiated k times before the

derivative becomes impulsive, has a frequency-domain excitation that falls off as $\Delta\omega^{-k}$ at appreciable offsets. This suggests that Gaussian pulses should provide an excitation pattern with one of the sharpest cutoffs in the tails. Gaussian shaping has proved to be a simple and widely applicable method for selective excitation in high-resolution spectroscopy. It is relatively easy to implement. A decision must be made as to the point at which the tails are truncated, usually between 1% and 5% of the peak intensity.

Another approach, much favored in magnetic resonance imaging, is to shape the pulse envelope according to a sinc function[29] since, in the Fourier approximation, this would give a rectangular or "top-hat" excitation profile. Intermediate between these cases lies the "Hermite" pulse[30] which is the product of a Gaussian and a polynomial. Hyperbolic secant pulses also have their advocates.[31]

B. Spin Pinging

Surprisingly enough, not all rectangular pulses necessarily involve a sinc function excitation pattern. If we prepare the spin system so that the initial condition for the selective pulse involves M_y rather than M_z, then the excitation pattern is far more favorable, having much weaker sidelobe responses. This experiment must be performed in a difference mode otherwise there are large signals off-resonance and the phase properties are unsuitable. The optimum flip angle for the selective pulse is π radians, carrying the on-resonance signal from the $+y$ to the $-y$ axis of the rotating frame. The experiment can be written as follows:

hard $(\pi/2)_x$ soft $(\pi)_x$ Acquire (+)

hard $(\pi/2)_x$ soft $(\pi)_y$ Acquire (−)

Suppose we start with a magnetization M_y after the initial hard $\pi/2$ pulse, at a general offset ΔB, with a transmitter level B_1, and a nominal flip angle α_0 for the soft pulse. We may define the parameters

$$\tan\theta = \Delta B/B_1 \qquad \alpha = \alpha_0 B_{eff}/B_1$$

$$B_{eff}^2 = \Delta B^2 + B_1^2$$

On this vector model, simple trigonometry shows that the dispersion-mode signals after both sequences are identical, equal to

$$M_y \sin\theta \sin\alpha$$

The dispersion contributions therefore disappear in the difference mode, whatever the resonance offset and whatever the soft pulse flip angle α_0. Consequently the excitation spectrum is in the pure absorption mode throughout.

More importantly, in the difference mode the frequency-domain excitation pattern has only very weak sidelobes, being described by

$$M_y = \tfrac{1}{2}M_0\alpha_0^2\left[\frac{\sin(\alpha/2)}{(\alpha/2)}\right]^2$$

whereas the corresponding expression for a single rectangular soft pulse has the form

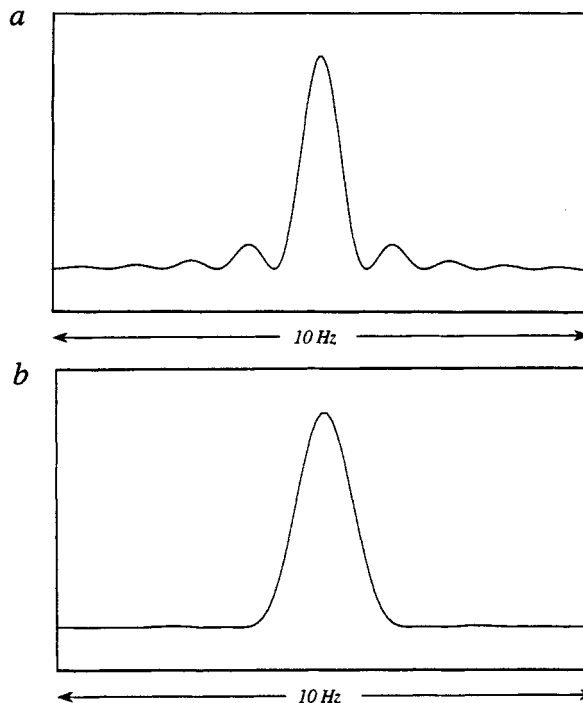$$M_y = M_0\alpha_0\left[\frac{[\sin(\alpha/2)]}{(\alpha/2)}\right]$$

Figure 11. Frequency-domain excitation profiles calculated for the "spin pinging" sequence, using (a) a rectangular soft pulse and (b) a soft pulse shaped according to an isoceles triangle. The soft pulse had a duration of 1 s.

The first expression, involving sinc^2, has much weaker sidelobe responses than the latter equation. Interestingly, this shape is retained for a wide range of values of the soft pulse flip angle α_0 (only the amplitude changes) implying that the method is extremely tolerant of pulse length miscalibration or spatial inhomogeneity of the B_1 field. This experiment has been called spin pinging;[32] a closely related technique was published simultaneously and independently by Canet[33] and called DANTE-Z. The excitation profile is easily improved still further by time-symmetric shaping functions applied to the soft pulse. For example, a time-domain envelope in the form of an isosceles triangle gives a frequency-domain profile described by a sinc^4 function, where the sidelobes are virtually undetectable. Figure 11 compares the frequency domain profiles calculated for spin pinging with a rectangular soft pulse and a triangular soft pulse.

C. Phase Gradients

There is one particular problem with many of the shaped pulses mentioned so far; they induce a strong variation in the phase of the excited signal across the selected region. This is easily visualized in the vector picture, since an off-resonance pulse causes a rotation about a tilted effective field in the rotating reference frame, carrying the appropriate vectors away from the zy plane toward the x axis (dispersion). The tilt angle increases with offset. Figure 12 shows a family of magnetization trajectories for increasing offsets from resonance. For the special case of a time-symmetric, amplitude-modulated pulse, the first-order approximation predicts that the resultant phase error is a linear function of offset. Pulse shapes that fall into this category include the Gaussian, Hermite, and sinc function pulses. For some applications, a linear phase
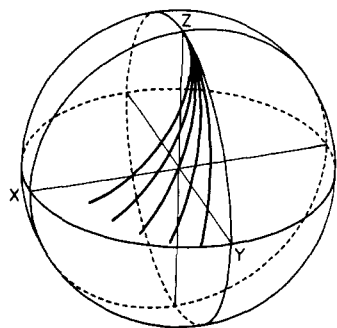
Figure 12. Magnetization trajectories for a soft pulse at increasing offsets from resonance. The effective field in the rotating frame tilts progressively further from the x axis toward the z axis, generating an increasing amount of dispersion mode signal (M_z).

Figure 13. Frequency-domain excitation profiles for a half-Gaussian selective pulse. The absorption-mode response is well-suited to selective coherence transfer experiments, but the dispersion-mode response has poor frequency selectivity.

dispersion may be corrected by conventional software routines before the spectrum is displayed, provided that the lines are sufficiently narrow in comparison with the rate of variation of phase with frequency. If not, then the line shapes are distorted and a "rolling base line" effect may be created. Alternatively, a refocusing method may be employed. In the case of magnetic resonance imaging experiments this can be achieved by reversing the applied field gradient. In high-resolution NMR a hard π pulse is used. Refocusing introduces its own problems. The additional delay causes signal loss through relaxation and allows time for the evolution of homonuclear couplings, giving rise to phase distortion within spin multiplets. The inevitable imperfections of the π pulses introduce undesirable magnetization components that have to be cancelled by a suitable phase cycle. Phase dispersion is therefore a serious problem. As these difficulties became more and more evident, it was recognized that pulse shapes needed to be specifically designed to match the requirements of the experiment, and if possible to excite the chosen region in the pure absorption mode with no frequency-dependent phase errors.

D. Half-Gaussian

It is somewhat misleading to assert that shaped pulses should have no sharp edges at all; it depends on what is to be observed. A pulse shaped according to the first half of a Gaussian curve[34] has important advantages for coherence transfer experiments where it is the absorption-mode profile that matters and where the dispersion signal is irrelevant. The phase gradient from a full Gaussian pulse may be thought of as arising because data acquisition starts late—at the end of the pulse rather that at the center. The half-Gaussian pulse greatly alleviates this problem by permitting data acquisition immediately after the peak, and the absorption mode excitation follows the same profile as that of a full Gaussian that has been corrected for its inherent phase gradient (the full curve of Figure 13). However the dispersion mode excitation is quite broad (the dashed curve of Figure 13). One way to visualize the action of a half-Gaussian pulse is to break it down into the sum of equal symmetric and antisymmetric parts (Figure 14). The antisymmetrical part excites dispersion-mode signals and, since it contains a large step discontinuity, accounts for the fact that the dispersion mode response covers a very wide frequency range. The symmetrical part excites absorption mode
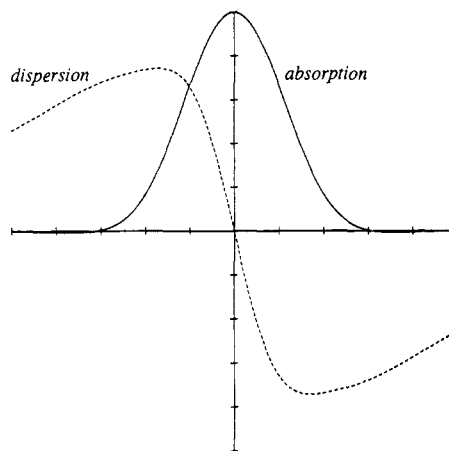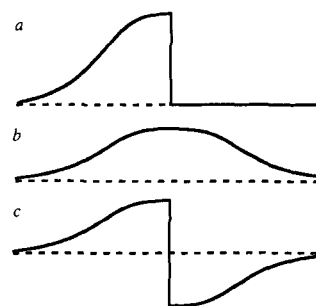

Figure 14. A half-Gaussian pulse (a) can be considered as the superposition of a symmetric full Gaussian (b), which excites the absorption-mode response, and an antisymmetric Gaussian (c), which excites the (broad) dispersion response.
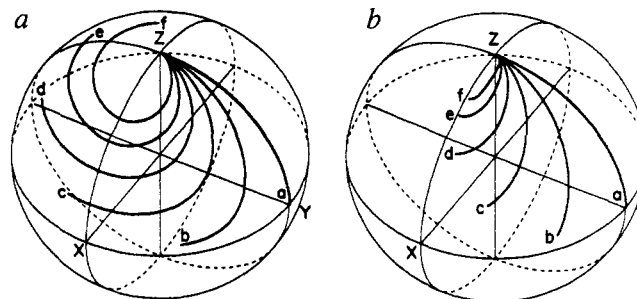

Figure 15. Magnetization trajectories calculated for a full Gaussian (a) and a half-Gaussian selective pulse (b). With the latter, the trajectories never reach the hemisphere where y is negative and there are no sidelobes on the excitation profile (reprinted from ref 34; copyright 1987 Academic Press).

signals and, having no discontinuity, gives an excitation profile with a monotonic cutoff in the tails, with no sidelobe responses. This behavior can be appreciated from the trajectories plotted in Figure 15 for a full Gaussian pulse and a half-Gaussian pulse of the same duration. Half-Gaussian trajectories never stray into the hemisphere where y is negative but they do have appreciable x components of magnetization.

In situations where the broad dispersion response must be eliminated, this can be achieved in a two-scan experiment with a hard $(\pi/2)$ purge pulse alternating along the $\pm y$ axes so as to cancel the undesirable x and z components of magnetization. This "purged half-Gaussian" pulse has been widely exploited for selective coherence transfer experiments.[35]

VI. Design of Pulse Shapes

We start from the most general theoretical description, the Liouville–von Neumann equation:

$$d\sigma/dt = -i[H, \sigma]$$

For the special case of a time-independent Hamiltonian, this has the solution

$$\sigma(t) = \exp(-iHt)\, \sigma(0)\, \exp(+iHt)$$

This is applicable to a pulse that has a rectangular envelope and no phase modulation, described (in the appropriate rotating frame) by the Hamiltonian

$$H = \Delta\omega I_z + \omega_1(I_x \cos \phi + I_y \sin \phi)$$

where ω_1 and ϕ are constant. We concentrate attention on the *propagator*

$$U = \exp(iH\tau)$$

where τ is the pulse duration. This propagator is independent of the initial state of the spin system. It can be written

$$U = \exp(-i\phi I_z)\, \exp(-i\theta I_y)\, \exp(-i\omega_{eff}\tau I_z)\, \exp(+i\theta I_y)$$
$$\exp(+i\phi I_z)$$

where the effective field is defined by

$$\tan \theta = \omega_1/\Delta\omega \quad \text{and} \quad \omega_{eff}^2 = \omega_1^2 + \Delta\omega^2$$

The propagator causes a rotation through an angle $\beta_0 = \omega_{eff}\tau$ about an axis $\mathbf{n}_0$

$$U = \exp[-i\beta_0(\mathbf{I}\cdot\mathbf{n}_0)]$$

where

$$\mathbf{n}_0 = [\omega_1(\mathbf{i} \cos \phi + \mathbf{j} \sin \phi) + \mathbf{k}\Delta\omega]/\omega_{eff}$$

that is to say an angle with direction cosines ($\omega_1 \cos \phi$, $\omega_1 \sin \phi$, $\Delta\omega$). (This is the result predicted by the usual vector model.) Its importance is that it provides the mechanism for treating the effect of a phase- and amplitude-modulated pulse by breaking down the pulse shape into a histogram made up of a regular sequence of rectangular pulses of differing amplitudes and phases. We define an *overall* propagator U_0, representing the net effect produced by the time-dependent Hamiltonian $H(t)$ over the course of the pulse.

$$\sigma(\tau) = U_0\sigma(0)U_0^{-1}$$

where U_0 is expressed as the product of unitary transformations

$$U_0 = U_N U_{N-1}...U_2 U_1$$

This overall propagator predicts the final density operator $\sigma(\tau)$ for any general initial condition $\sigma(0)$.

An alternative approach is to calculate the *average Hamiltonian* H^* for the shaped pulse, defined by

$$U_0 = \exp(-iH^*\tau)$$

This represents the overall effect of the general time-dependent Hamiltonian over the pulse width τ. The computation is more extensive, involving numerical diagonalization of the matrix U_0, taking logarithms of
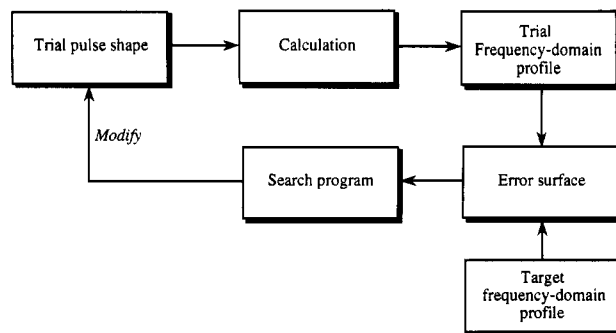

Figure 16. Computer scheme for designing shaped pulses to achieve a predefined target excitation profile.

the resulting eigenvalues and transforming back into the original reference frame. For certain applications it is sufficient to perform an approximate calculation of the average Hamiltonian through the Magnus expansion.[36]

A. The Inverse Problem

These calculations tell us how to evaluate the effect on the spin system of a pulse of known shape. They do not solve the inverse problem of designing a pulse shape to achieve a predefined excitation pattern. This much more demanding problem requires iterative numerical procedures. It was the practitioners of magnetic resonance imaging who first made use of "designer pulses" for selective excitation and there is an extensive literature on the subject.[37-46] High-resolution spectroscopists were initially quite content to use simple pulse shapes like the Gaussian[28] since phase dispersion is more easily corrected in spectra made up of several discrete narrow lines.

To design a pulse for a particular excitation profile and pure absorption mode, the first step is to specify a trial pulse shape in terms of a suitable set of parameters. This could be a simple set of discrete phase and intensity values at regular time intervals—the point-by-point definition. The problems with this method are that the number of parameters can be very high and that it is necessary to ensure (by other constraints) that the pulse envelope remain continuous. A polynomial expansion provides an alternative method for defining pulse shape, providing continuity and a restricted parameter set. A finite Fourier series expansion has proved to be a rewarding approach.[46,47] Not only does it keep the number of parameters small, but also it ensures that the pulse shape is continuous. By introducing higher order Fourier coefficients gradually and conservatively, we can ensure that the pulse envelope remains as simple as possible. Some of the rival methods can generate extremely convoluted shapes that are difficult to implement in practice and are quite intolerant of instrumental imperfections.

Iterative methods use the forward calculation to compute an excitation profile for a given trial pulse shape, compare this with the predefined target profile and then modify the pulse shape parameters to give a better approximation to the target. Figure 16 is a schematic diagram of this procedure. Essentially this is a search over a multiparameter error surface to find the optimum solution. There are several conventional "gradient descent" routines to do this. The difficulties arise when there are several minima on the error surface

and the program finds only a "local" rather than "global" minimum. Later we examine three approaches to pulse design conceived to circumvent this problem.

B. General Rotation Pulses

So far we have made the tacit assumption that the pulse acts on magnetization at equilibrium along the z axis. This, of course, is not always the case. For example, in a spin echo refocusing experiment we need to perform a π rotation for magnetization vectors in the xy plane with any arbitrary phase, and several multidimensional experiments require a general $\pi/2$ rotation for vectors at arbitrary positions. We call these "general rotation pulses" and their action is a rotation through β radians, independent of the initial condition of the nuclear magnetization. This is a much more challenging problem that finding a pulse that rotates *longitudinal* magnetization. It involves discovering a "propagator" representing a constant rotation through β radians, corresponding to an average Hamiltonian $H^* = (\beta/\tau)I_x$. To design a general rotation pulse, the pulse shape is adjusted iteratively until the average Hamiltonian fits the target function. The design of general rotation $\pi/2$ and π pulses has been described in some detail.[47]

C. Evolutionary Methods

A careful study of the processes of nature may often help us solve technological problems. A good example is the adaptation of Darwin's concept of natural selection, which governs evolution, to solve complex problems of aerodynamic engineering.[48] In nature, small genetic variations are favored if this renders the offspring better adapted to its environment. In a sense each individual genetic change is a random process, but the cumulative effect of a long sequence of such changes becomes directed and accounts for the driving force behind the evolution of all living organisms. The same concept may also be applied to magnetic resonance problems.[49] The numerical values of the physical parameters are thought of as "genes" which can be incremented ("mutation") to produce several trial solutions ("offspring"), one of which is chosen to be the starting point ("parent") of the next "generation". A hostile "environment" is provided by a computer program which encourages changes that appear to favor the overall target of the project, for example a shaped selective pulse. Evolutionary algorithms based on these principles are well established in many areas of science and engineering.

We may introduce a radical modification of this classic evolutionary scheme by replacing the computer by a skilled NMR spectroscopist at the critical stage where the choice is made between offspring. This is not merely a simplification of the algorithm, but changes the very nature of the process, since a human operator is much better at pattern recognition and much more flexible about goals. Indeed, there is now no longer any necessity for a precise target function since the spectroscopist may work with much more broadly conceived aims than the computer algorithm, indeed he may vary these goals as the search proceeds. No formal error function is computed; we may therefore question whether this should be described as an *optimization* procedure at all. The NMR spectroscopist simply makes his choice, using intuition, lateral thinking, ex-
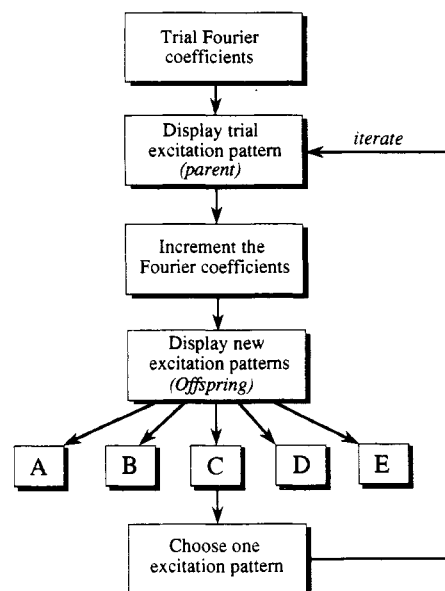

Figure 17. Schematic representation of the evolutionary method used to design pulse shapes. The "genes" in this case are coefficients in a finite Fourier series used to define the pulse envelope.

pert judgement, or just plain guesswork to "guide" the program along what appears to be a useful evolutionary path. Not every choice need be demonstrably productive.

In practice the computer monitor displays frequency-domain excitation patterns that represent the parent and several offspring.[50,51] The process is illustrated schematically in Figure 17. The operator chooses one of the patterns to be the parent of the next generation, nudging the evolution along what appears to be a productive direction. He need not always make a wise choice, indeed there may be something to be said for an occasional whimsical variation of the genes to direct the program in an entirely different direction. This is certainly not a blind mechanical search for an optimum solution. Evolution space is a branching network, and every time the operator makes a choice, he eliminates millions of possible outcomes. In this sense evolution resembles the game of chess where a score of moves is enough to create unprecedented positions on the board. We could even speculate that such an interactive scheme might one day discover a completely new result not anticipated when the problem was first formulated, provided that the spectroscopist keeps an open mind and is always on the look-out for the emergence of novel solutions. It would be difficult indeed to program a computer to achieve this. Guidance by a skilled spectroscopist is therefore a crucial modification of the evolutionary method.

As an example, consider the problem of generating a shaped broad-band excitation pulse. The requirement would be uniform excitation in the pure absorption mode over a predefined *effective bandwidth*, with negligible dispersion mode excitation. Outside this effective bandwidth we allow any arbitrary excitation behavior so this is not strictly a band-selective pulse. Although a sufficiently hard pulse can accomplish a similar result, there can be situations where a weak shaped pulse might be preferable. Starting with trial pulse shape parameters in the form of the coefficients of a finite Fourier series, an evolution program was
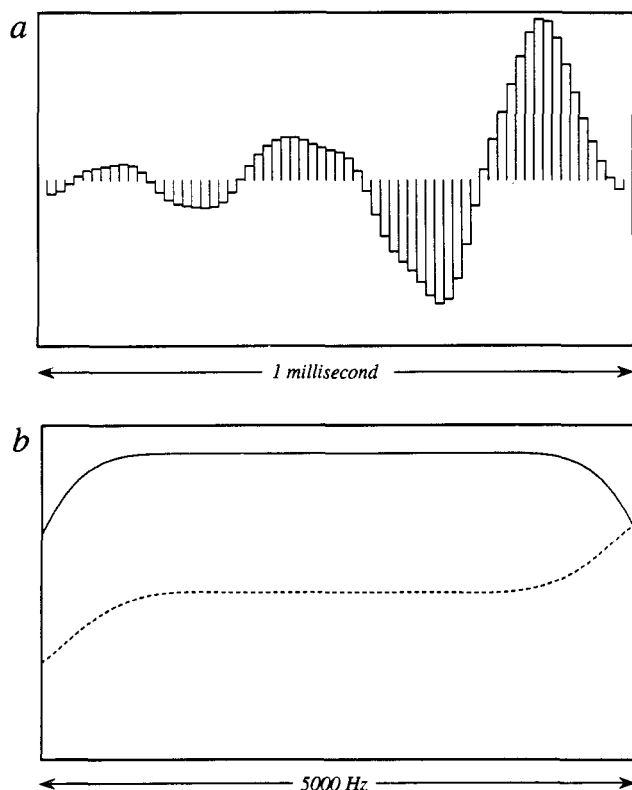
Figure 18. A shaped pulse (a) designed to give a broadband excitation profile (b) with uniform absorption (full curve) and negligible dispersion (dashed curve) across a 4000-Hz bandwidth. It was designed by the evolutionary method used Fourier coefficients as the variable parameters (reprinted from ref 51; copyright 1991 Academic Press).

written where each set of new frequency-domain profiles could be displayed on a computer monitor. These may all be regarded as the direct offspring of a previous result. The operator examines each profile for desirable characteristics (flatter absorption profile, lower dispersion profile) at the same time rejecting any tendency toward artifactual responses. The pulse shape corresponding to this selected response acts as the parent for the next generation. A human operator, particularly an experienced NMR spectroscopist, can make a complex set of value judgements about each pattern displayed on the screen, and may even change the target of the search if something interesting crops up. This broad-band excitation pulse shape was in fact discovered as a byproduct of a quite different search.[51] Figure 18 shows the pulse shape and frequency-domain excitation profile of this broad-band pulse. The absorption-mode signal is uniform within ±0.0006 over a 3000-Hz band while the phase is constant to within ±0.5° (something that would be very difficult to achieve with a conventional hard pulse).

D. Neural Networks

We can imagine a situation in magnetic resonance imaging and in vivo spectroscopy where the physicians have obtained an image and wish to record a high-resolution spectrum from some irregularly shaped organ within the patient. This requires the design of suitably shaped localized excitation pulses *on the spot*, that is to say, with the least possible delay for the computation. Here is one of the principal advantages of the method
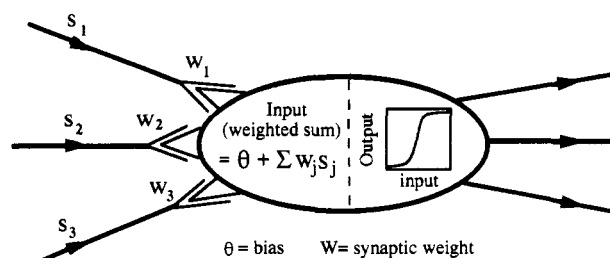

Figure 19. Schematic diagram of a neuron as used in the simulated neural network. Several input signals are combined as a weighted sum, "amplified" according to a sigmoid response with a bias θ, and passed on to other neurons "downstream".
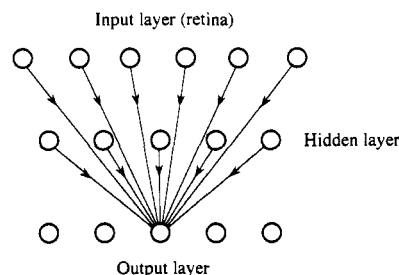

Figure 20. Schematic diagram of a three-layer neural network. Each neuron in the final layer receives signals from all neurons in the first two layers.

of neural networks—the actual calculation is quite rapid compared with the much longer time taken to "train" the network for its task. A neural network mimics the way the brain is believed to work, by simulation on a digital computer.[52] A neuron is represented schematically in Figure 19. There are several inputs controlled in amplitude by the synaptic weights W_j. The weighted signal voltages are summed and converted by the sigmoid response function with a bias θ to give a common output which is then fed to several more neurons "downstream".

The network is constructed in several layers. Input is received by the first layer (the "retina"). A neuron in an intermediate layer receives signals from all neurons in the retina, summing them with the appropriate "synaptic weights" and "biases", passing the resultant to neurons in the next layer. In practice three layers appear to suffice for the pulse shaping application and "feedback" to earlier layers is not required. The final layer receives signals from both the retina and the intermediate layer (Figure 20) and generates the signals that will eventually represent the pulse-shape parameters (Fourier coefficients) corresponding to the input excitation pattern. This is achieved in the "training mode" (Figure 21). Starting with a series of randomly generated trial pulse shapes, the program calculates the corresponding frequency-domain excitation profiles and feeds these to the retina one at a time. Initially the synaptic weights and biases are quite random and there is no correlation at all between output and input. Each set of output Fourier coefficients is compared with those of the corresponding trial pulse shape, and changes are made to the synaptic weights and biases to improve the fit. Thus very gradually, as different trial patterns are presented to the retina, the network "learns" to recognize them and generates a better and better approximation to the corresponding pulse shape. This acquired "knowledge" resides in the values of the synaptic weights and the biases associated with each neuron.
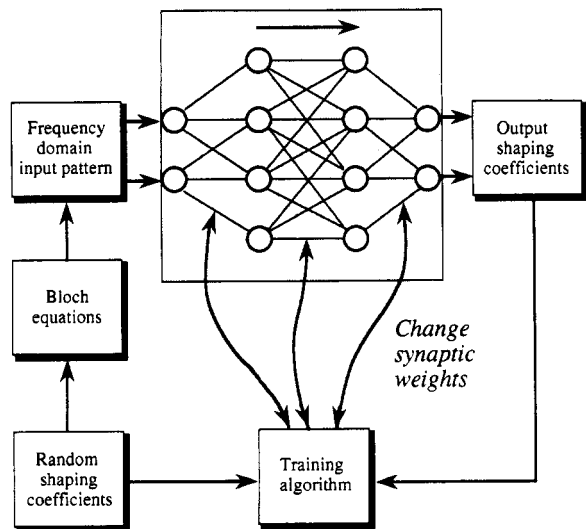
Figure 21. The training mode of a neural network used to design pulse shapes. Randomly generated pulse shapes are converted into the corresponding frequency domain excitation profiles and presented to the retina. The control program readjusts biases and synaptic weights within the network to bring the output shaping coefficients closer to the trial coefficients.
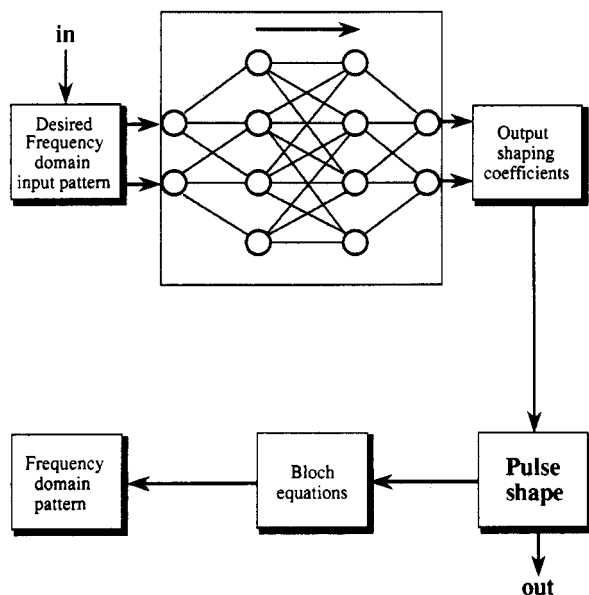

Figure 22. Once the neural network has been suitably trained, it is switched to the operating mode. Presentation of a desired excitation profile to the retina results in outputs that are a good approximation to the Fourier coefficients required to shape the pulse.

This training mode can be very protracted since each individual presentation to the retina involves solving (say) the Bloch equations for each trial pulse shape. The trial shapes should of course be planned to cover the entire range of conditions that may be anticipated when the network is changed to its operating mode.

The operating mode works much more rapidly (Figure 22). A presentation of the required frequency domain pattern to the retina is followed soon afterward by a set of Fourier coefficients at the output layer. The long training schedule has paid off by adapting the synaptic weights and biases so that it can now perform the calculation without knowing the result in advance. We have built a machine that can invert the Bloch equations. It is quite possible that a sportsman, by
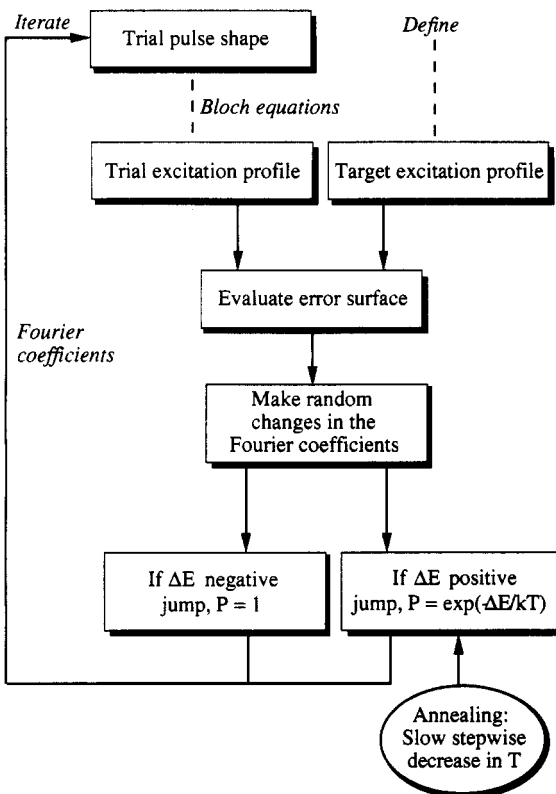

Figure 23. Simulated annealing scheme for designing shaped pulses. The key feature is the slow stepwise reduction in T.

repeated training, learns to perform (say) the high jump by a broadly analogous mechanism.

A practical test of design of pulse shapes by a neural network proved quite encouraging.[53] The target was to design a pulse which, applied to a J doublet, excited antiphase magnetization $(2I_xS_z)$ uniformly over a range of possible J values. This "JANUS" pulse should be a useful first stage in many coherence transfer experiments.

E. Simulated Annealing

The pitfalls of conventional gradient descent routines are neatly avoided by the method known as simulated annealing,[46,54] based on an analogy with the annealing of a metal. As before, the problem is parametrized, for example in terms of the Fourier coefficients that define the pulse shape, and an error function is defined in terms of the mean square deviations between the trial and target excitation profiles (Figure 23). Small random changes are made to each parameter in turn to find out whether the error function increases or decreases. In this search for the global minimum on the multidimensional error surface, the program normally moves "downhill" but occasionally accepts an "uphill" jump to a point with a higher mean square error. The idea is to avoid becoming trapped in a local minimum that does not represent the optimum solution. Uphill jumps are only permitted with a low probability, $\exp(-\Delta E/kT)$, whereas downhill jumps are always implemented. This "Boltzmann" factor involves the change in the error function ΔE, and a parameter T which can be thought of as temperature. Thus any variation in the Fourier coefficients which causes a large increase in the mean square error is very unlikely to be allowed, the more so the lower the temperature T. The art lies in

the manner in which the temperature is lowered—the annealing schedule. At high temperatures, uphill and downhill moves are about equally probable and the error surface can be thoroughly explored without danger of becoming trapped in a local minimum. Small stepwise reductions in temperature are then made, with more and more time allowed at each level as the program proceeds. Gradually the search finds minima on the error surface but retains enough "kinetic energy" to escape them and explore other regions until the global solution is finally discovered. The key to a successful simulated annealing run is to choose the best compromise between cooling too fast (quenching) and cooling too slowly (which would use too much computer time). When a global solution is located, it is often advantageous to refine the parameters by conventional gradient descent methods for these are much faster.

VII. Band-Selective Pulses

Simulated annealing has proved its worth in the search for a shaped pulse which excites across a selected frequency region with uniform intensity and pure absorption phase. This supposes a built-in compensation for the phase gradients inherent in most other selective pulses. It was not obvious a priori that this goal of "self-focusing" could be achieved by amplitude modulation alone. (In fact it has been speculated[55] that purely amplitude-modulated self-focusing pulse shapes will not be easily implemented and are therefore of little practical importance, implying that the solution should be sought for pulses with both phase and amplitude modulation.) Outside the prescribed bandwidth (and a narrow transition region) the excitation should be negligible. In the event, simulated annealing calculations produced a family of these band-selective, uniform response, pure-phase (BURP) pulses suitable for excitation, coherence transfer, population inversion, and refocusing.[47,56,57]

The need arose for band-selective pulses due to the very high information content of present-day high-resolution spectrometers. The problem is compounded for multidimensional spectroscopy. For example, a three-dimensional experiment with a thousand data points in each dimension and with evolution and acquisition times of 0.2 s would require *one week* of data accumulation (not counting extra relaxation delays or computer housekeeping) and a data matrix of *one billion* words. The requirements of the Nyquist sampling condition normally preclude the narrowing of the spectral widths since aliasing cannot be tolerated in most chemical applications. However if the *excitation* bandwidths are reduced then the sampling rates, the size of the data matrix, and the experimental time can all be correspondingly reduced. Even a halving of the excitation bandwidth gives an 8-fold reduction in the size of the data table. Band-selective pulses can achieve this.

One representative example is the band-selective "BURP" pulse which has the pulse shape and excitation profile illustrated in Figure 24. As a test for its "pure-phase" behavior and the suppression of signals outside the specified band, the spectra shown in Figure 25 were recorded. A section of the 400-MHz proton spectrum of strychnine was examined one spin multiplet at a time, with no readjustment of the spectrometer
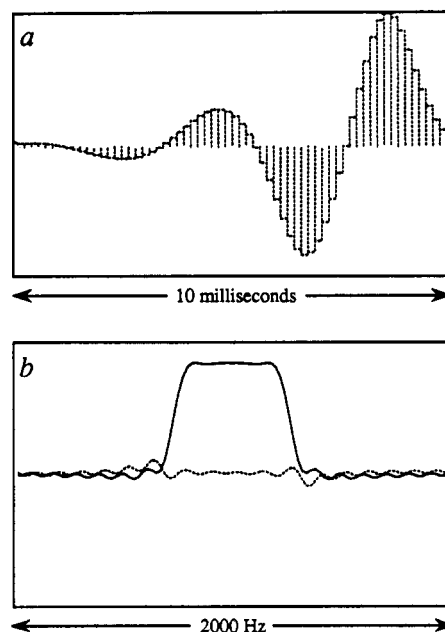

Figure 24. Pulse shape (a) and excitation profile (b) for the band-selective pulse E-BURP-2. The full curve represents the absorption mode and the dashed curve the dispersion mode. The selectivity can be increased by increasing the pulse length (reprinted from ref 47; copyright 1991 Academic Press).
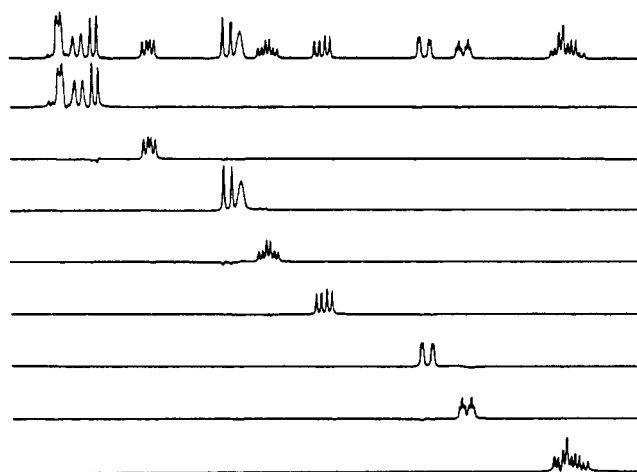

Figure 25. Part of the 400-MHz proton spectrum of strychnine. The lower traces show the selective excitation of the spin multiplets one at a time using the E-BURP pulse. Note particularly the pure absorption phase and the lack of distortion compared with the full spectrum. No phase corrections were made within the series.

phase controls within the series. An essentially undistorted version of each multiplet is reproduced with little residual signal from adjacent multiplets. In each case the signals are in the pure absorption mode. Pulses from this family should prove very useful for multidimensional spectroscopy.

VIII. Applications of Selective Pulses

There is now a large number of selective pulse experiments in the literature and a comprehensive survey would be beyond the scope of this review. However, some valid generalizations can be made. These new selective schemes are often derived from existing hard-pulse experiments simply by replacing one or more hard pulses by soft pulses. The aim may be to simplify

the spectrum, confirm an assignment, reduce the dimensionality, or improve sensitivity or the fineness of digitization. Alternatively, we may attack a specific instrumental problem such as that posed by very intense solvent peaks, although this demands a very high level of suppression indeed and most shaped pulses are not well-suited to this application.

A. Simplification and Assignment

One early example serves to illustrate this concept. Long-range carbon–proton couplings are notoriously difficult to detect and assign. In the proton spectrum they are often obscured among the small artifact responses in the flanks of the intense proton signal from carbon-12 molecules; in the carbon-13 spectrum the multiplets can be quite complicated and the wide spectral widths often preclude the examination of the finer details of spin multiplet structure. A simple modification of the conventional heteronuclear two-dimensional J spectrum provides the key.[58] The usual hard proton 180° refocusing pulse is replaced by a soft pulse at a particular proton chemical shift frequency (δ_A) with selectivity of the order of 25 Hz. This restricts the spin-echo modulation to a single component at the frequency of the long-range proton–carbon coupling constant. The outer satellite lines due to the direct proton–carbon coupling are too far away to be affected, but the inner satellites are inverted by the soft pulse. The result is a particularly simple carbon-13 spectrum (doublet, triplet, or quartet) with good digital definition, since the F_1 spectral width can be as narrow as ±10 Hz. The assignment is direct and unambiguous, based on the choice of the proton frequency δ_A. The sensitivity is quite high, for although a two-dimensional spectrum can lose some sensitivity with respect to the corresponding one-dimensional analogue, not many t_1 increments need to be involved here, and there is a considerable reduction in the number of times the carbon-13 resonance is split. Of course each site has to be investigated separately, and some sites may not be accessible owing to overlap of neighbor resonances. This is a good illustration of how an existing experiment can be radically changed by the substitution of a soft pulse for a hard pulse.

B. Reduction of Dimensionality

Although two-dimensional spectroscopy has enjoyed unprecedented success, not all problems are best solved by this method, particularly where close attention to the detailed fine structure is the prime goal. There is now a vast family of investigations in which a two-dimensional hard-pulse experiment has been converted into a soft-pulse one-dimensional version. Sheer volume of information is thereby traded for wealth of fine detail. In fact it is often in cases where the two-dimensional spectrum is very crowded that the soft-pulse experiment shows its true worth.

We can take a very early experiment to illustrate this principle.[28] A conventional homonuclear shift correlation experiment (COSY) can be converted into a small number of one-dimensional experiments if the initial excitation pulse is a soft Gaussian (of the order of 100 ms duration) centered on a chosen spin multiplet. In this experiment the usual evolution period t_1 is replaced by a fixed interval τ and this is followed by a hard $\pi/2$
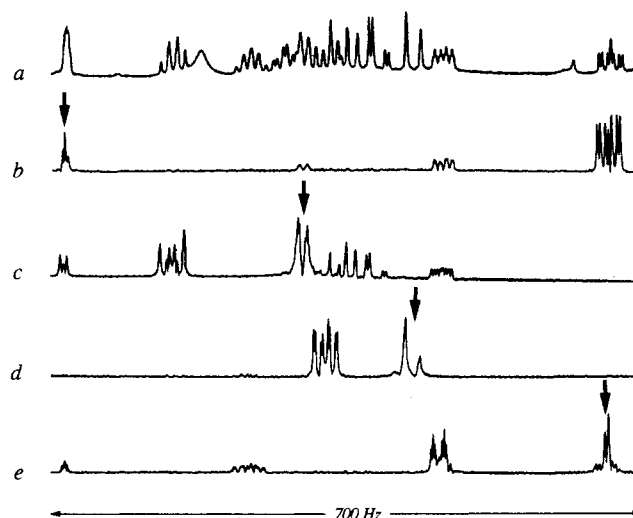

Figure 26. Selectively excited one-dimensional correlation spectra of protons in a tricyclodecanone derivative: (a) conventional spectrum; (b–c) coherence transfer spectra. Gaussian-shaped excitation pulses were applied at the frequencies marked by the arrows (reprinted from ref 28; copyright 1984 Academic Press).

pulse. Coherence is transferred to all directly coupled sites with an intensity dependent on τ and the appropriate J coupling. Since we are at liberty to choose a well-isolated multiplet for excitation, this technique may be used to probe overlapping responses by transferring coherences selectively into the crowded region. Figure 26 shows some of these "one-dimensional-COSY" traces obtained in the crowded spectrum of protons in a tricyclodecanone derivative.

C. Crowded Two-Dimensional Spectra

As more and more complicated molecules are investigated by two-dimensional spectroscopy, congestion becomes a common problem. Cross-peaks are crowded together and overlap, obscuring useful fine structure information. Sometimes a "surgical" line-selective soft-pulse experiment can dissect the overlapping components. An illustrative example is provided by a scheme to separate overlapping cross-peaks in homonuclear correlation (COSY) spectra. In most practical cases the overlap is seldom complete. Even where one cross-peak is engulfed by the other, there is usually an F_1 frequency to be found that slices through one and not the other. In favorable cases this might be the extreme edge of one cross-peak, but this is not a necessary condition for success.

The technique can be demonstrated by using the spin pinging sequence[32] for selective excitation of one line in the F_1 dimension of a COSY experiment. If any line of a given spin multiplet is excited in this way, the next hard $\pi/2$ pulse has the effect of spreading the excitation throughout all the lines of that multiplet. Coherence is then transferred as a COSY experiment with a variable evolution period followed by a hard $\pi/2$ pulse. A second experiment, attacking a single transition of the second (overlapped) multiplet, allows the two to be recorded separately. Figure 27 shows such a decomposition in the correlation spectrum of protons in a biosynthetically generated copolymer. This has four overlapping cross-peaks. By judicious choice of excitation frequencies each cross-peak has been separately recorded.[59]
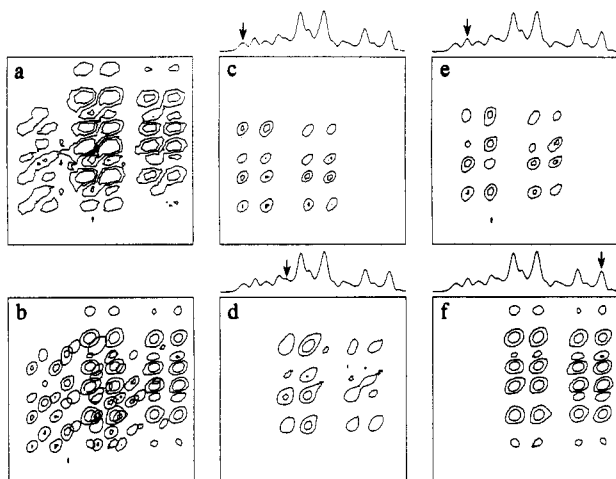
Figure 27. Separation of four overlapping cross-peaks in the COSY spectrum of a copolymer by line-selective excitation with the spin pinging sequence: (a) the composite cross-peak from the conventional COSY spectrum; (c–f) the individual cross-peaks separated by excitation at the frequencies indicated by the small arrows; (b) superposition of c, d, e, and f for comparison with a (reprinted from ref 59; copyright 1990 Academic Press).

D. Three-Dimensional Spectroscopy

Multidimensional spectra make enormous demands on overall experimental time and computer data storage space. This may preclude a careful examination of the fine structure of cross-peaks, since there is neither time nor space to employ a large number of samples in each time dimension. An interesting alternative is a direct exploration of two frequency dimensions with line-selective pulses,[60] using Fourier transformation only for the final (acquisition) dimension. A complete step-by-step examination of one frequency dimension (F_1) is made for each step in the second dimension (F_2). Although this two-dimensional search could be laborious, the experiment is redeemed by greatly restricting the frequency ranges so as to encompass only the desired cross-peak. The frequency increments are chosen to correspond to the selectivity of the soft pulses. As an illustration, Figure 28 shows a three-dimensional cross-peak response from protons in acrylic acid recorded in this manner. It contains four quartets, each with a (+ – – +) or (– + + –) pattern of intensities running parallel to the F_3 dimension. It maps out a volume of frequency space 18.6 Hz × 11.8 Hz × 27.6 Hz.

IX. Conclusions

In the 1960s, the concept of selective excitation received little attention (except in terms of double resonance experiments) for virtually all spectra were excited selectively, the frequency being swept to pass from one resonance to the next. We have seen that the conversion to Fourier transform methods generated a new need for experiments with selective pulses. At first these were implemented in the simplest possible fashion, by lengthening the pulse and lowering the B_1 level accordingly, but it became apparent that the sharp rising and falling edges of the pulse introduced undesirable sidelobe features into the excitation spectrum. The remedy was to shape the pulse, initially by means of simple analytical functions such as the Gaussian, but eventually by carefully designed functions calculated
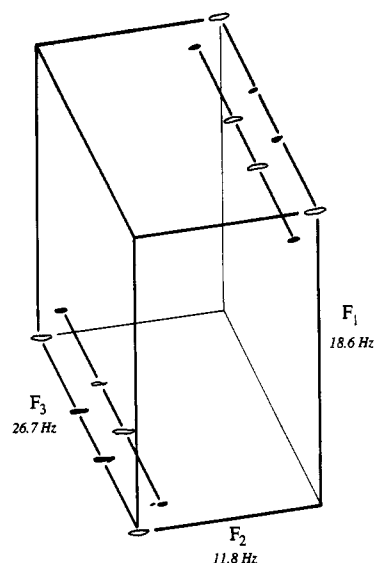

Figure 28. A three-dimensional cross-peak from the proton spectrum of acrylic acid obtained by scanning the F_1 and F_2 frequency dimensions with line-selective pulses. The F_3 dimension was recorded by the conventional Fourier transform method. Negative responses are shown as filled contours (reprinted from ref 60; copyright 1988 Taylor & Francis).

to achieve a specific frequency-domain profile. It is indeed rather surprising that a purely amplitude modulated pulse can be designed not only to be band selective, but also to have uniform intensities and pure absorption mode signals across the prescribed operating bandwidth. No doubt even higher levels of sophistication in pulse design may be anticipated in the future.

References

(1) Alexander, S. *Rev. Sci. Instrum.* **1961**, *32*, 1066.
(2) Freeman, R.; Wittekoek, S. *Proceedings of the 15th Colloque Ampere*, Grenoble North Holland Publishing Co.: Amsterdam, 1968.
(3) Freeman, R.; Wittekoek, S. *J. Magn. Reson.* **1969**, *1*, 238–276.
(4) Forsén, S.; R. A. Hoffman, R. A. *J. Chem. Phys.* **1963**, *39*, 2892.
(5) Ernst, R. R.; W. A. Anderson, W. A. *Rev. Sci. Instrum.* **1966**, *37*, 93.
(6) Vold, R. L.; Waugh, J. S.; Klein, M. P.; Phelps, D. E. *J. Chem. Phys.* **1968**, *48*, 3831.
(7) Patt, S. L.; Sykes, B. D. *J. Chem. Phys.* **1972**, *56*, 3182.
(8) Redfield, A. G.; Kunz, S. D.; Ralph, E. K. *J. Magn. Reson.* **1975**, *19*, 114.
(9) Meiboom, S.; Gill, D. *Rev. Sci. Instrum.* **1958**, *29*, 688.
(10) Freeman, R.; Hill, H. D. W.; Tomlinson, B. L.; Hall, L. D. *J. Chem. Phys.* **1974**, *61*, 4466–4473.
(11) Freeman, R.; Wittekoek, S.; Ernst, R. R. *J. Chem. Phys.* **1970**, *52*, 1529–1544.
(12) Mayne, C. L.; Alderman, D. W.; Grant, D. M. *J. Chem. Phys.* **1975**, *63*, 2514.
(13) Carr, H. Y.; Purcell, E. M. *Phys. Rev.* **1954**, *94*, 630.
(14) Solomon, I. *C. R. Acad. Sci. Paris* **1959**, *248*, 92.
(15) Solomon, I. *Phys. Rev. Lett.* **1959**, *2*, 301.
(16) Plateau, P.; Guéron, M. *J. Am. Chem. Soc.* **1982**, *104*, 7310.
(17) Sklenar, V.; Starcuk, Z. *J. Magn. Reson.* **1982**, *50*, 495.
(18) Turner, D. L. *J. Magn. Reson.* **1983**, *54*, 146.

(19) Hore, P. J. *J. Magn. Reson.* **1983**, *54*, 539.
(20) Hore, P. J. *Meth. Enzymol.* **1989**, *176*, 64–77.
(21) Bax, A.; Freeman, R. *J. Magn. Reson.* **1980**, *37*, 177–181.
(22) Bodenhausen, G.; Freeman, R.; Morris, G. A. **1976**, *23*, 171–175.
(23) Morris, G. A.; Freeman, R. *J. Magn. Reson.* **1978**, *29*, 433–462.
(24) Geen, H.; Wu, X. L.; Xu, P.; Friedrich, J.; Freeman, R. *J. Magn. Reson.* **1989**, *81*, 646–652.
(25) Morris, G. A.; Freeman, R. Unpublished results.
(26) Tomlinson, B. L.; Hill, H. D. W. *J. Chem. Phys.* **1973**, *59*, 1775.
(27) Sutherland, R. J.; Hutchinson, J. M. S. *J. Phys. E.: Sci. Instrum.* **1978**, *11*, 79.
(28) C. Bauer, C.; Freeman, R.; Frenkiel, T.; Keeler, J.; Shaka, A. J. *J. Magn. Reson.* **1984**, *58*, 442.
(29) Silver, M. S.; Joseph, R. I.; Hoult, D. I. *Magn. Reson.* **1984**, *59*, 347.
(30) Warren, W. S. *J. Chem. Phys.* **1984**, *81*, 5437.
(31) Baum, J.; Tycko, R.; Pines, A. *Phys. Rev.* **1985**, *A32*, 3435.
(32) Wu, X. L.; Xu, P.; Freeman, R. *J. Magn. Reson.* **1989**, *83*, 404–410.
(33) Boudot, D.; Canet, D.; Brondeau, J.; Boubel, J. C. *J. Magn. Reson.* **1989**, *83*, 428–439.
(34) Friedrich, J.; Davies, S.; Freeman, R. *J. Magn. Reson.* **1987**, *75*, 390–395.
(35) Kessler, H.; Anders, U.; Gemmecker, G.; Steuernagel, S. *J. Magn. Reson.* **1989**, *85*, 1.
(36) Magnus, W. *Commun. Pure Appl. Math.* **1954**, *7*, 649.
(37) Lurie, D. J. *Magn. Reson. Imaging* **1985**, *3*, 235.
(38) O'Donnell, M. *Magn. Reson. Imaging* **1985**, *3*, 377.
(39) Connolly, S.; Nishimura, D.; Macovski, A. *IEEE Trans. Med. Imaging* **1986**, *M15*, 106.
(40) Ngo, T.; Morris, P. G. *Biochem. Soc. Trans.* **1986**, *14*, 1271.
(41) Murdoch, J.; Lent, A. H.; Kritzer, M. *J. Magn. Reson.* **1987**, *74*, 226.

(42) Bendall, M. R.; Garwood, M.; Ugurbil, K.; Pegg, D. T. *Magn. Reson. Med.* **1987**, *4*, 493.
(43) Andrew, E. R.; Latanowicz, L. *J. Magn. Reson.* **1986**, *68*, 232.
(44) Loaiza, F.; McCoy, M.; Silver, M.; Warren, W. S. *Proc. N.Y. Acad. Sci.* **1988**, *508*, 483.
(45) Warren, W. S.; Silver, M. S. *Adv. Magn. Reson.* **1988**, *12*, 247.
(46) Hardy, C. J.; Bottomley, P. A.; O'Donnell, M.; Roemer, P. *J. Magn. Reson.* **1988**, *77*, 233.
(47) Geen, H.; Freeman, R. *J. Magn. Reson.* **1991**, *93*, 93.
(48) Rechenberg, I. *Evolutionsstrategie: Optimierung Technische Systeme nach Prinzipien der Biologischen Evolution*; Frommann-Holzboog: Berlin, 1973.
(49) Loaiza, F.; Lim, K. T.; Warren, W. S.; Silver, M.; Egloff, H.; Kiefer, B.; Laub, G. *Health Care Instrum.* **1986**, *1*, 188.
(50) Freeman, R.; Wu, X. L. *J. Magn. Reson.* **1987**, *75*, 184–189.
(51) Xu, P.; Wu, X. L.; Freeman, R. *Magn. Reson. Med.* **1991**, *20*, 165–170.
(52) Rosenblatt, F. *Principles of Neurodynamics: Perceptrons and the Theory of Brain Mechanisms*; Spartan Books: Washington, DC, 1961.
(53) Gezelter, J. D.; Freeman, R. *J. Magn. Reson.* **1990**, *90*, 397–404.
(54) Metropolis, N.; Rosenbluth, A. W.; Rosenbluth, M. N.; Teller, A. H.; Teller, E. *J. Chem. Phys.* **1953**, *21*, 1087.
(55) Loaiza, F.; McCoy, M.; Hammes, M. S.; Warren, W. S. *J. Magn. Reson.* **1988**, *77*, 175.
(56) Geen, H.; Wimperis, S.; Freeman, R. *J. Magn. Reson.* **1989**, *85*, 620–627.
(57) Geen, H.; Freeman, R. *J. Magn. Reson.* **1990**, *87*, 415–421.
(58) Bax, A.; Freeman, R. *J. Am. Chem. Soc.* **1982**, *104*, 1099–1100.
(59) Xu, P.; Wu, X. L.; Freeman, R. *J. Magn. Reson.* **1990**, *89*, 198–204.
(60) Friedrich, J.; Davies, S.; Freeman, R. *Mol. Phys.* **1988**, *64*, 691–713.